Supplementary Information (SI) for Journal of Materials Chemistry A.

Supplementary Materials

Fabrication of graphene oxide/silk protein core-sheath aerogel fibers for thermal management

Experimental

1 Materials

The graphite powder used in this study was purchased from Qindao Tengshengda Carbon Machinery Co., Ltd.; nitric acid, sodium carbonate, concentrated sulfuric acid, hydrogen peroxide, and N,N-dimethylformamide (DMF) were supplied by Fengchuan Chemical Reagent Technology Co., Ltd., Tianjin; potassium permanganate was obtained from Changhua Bio-Tech Co., Ltd.; concentrated hydrochloric acid was purchased from Gu'an Jinlian Fine Chemicals Development Co., Ltd.; mulberry cocoons were supplied by Bozhou Haoyihuang Bio-Tech Co., Ltd.; dialysis bags with a molecular weight cut-off of 14,000 Da and a pore size of 5 nm were used; polyethylene glycol (PEG, molecular weight 4000) was acquired from China National Pharmaceutical Group Chemical Reagents Co., Ltd.; and TPU pellets (model 1185A) were provided by BASF Germany. The co-axial spinneret, featuring an inner diameter of 0.4 mm (22G) and an outer diameter of 1.05 mm (17G), was supplied by Jintou Mechanical Processing Center in Gu'an County. All the materials were used without further purification.

2 Fabrication of GO/SF@TPU composite aerogel fibers

2.1 Synthesis of GO

GO was synthesized using a modified Hummers method.[1]

2.2 Preparation of SF solution

Mulberry cocoons were boiled in a 0.5 wt.% aqueous solution of sodium carbonate (Na_2CO_3) to remove sericin proteins. Purified silk fibers were then thoroughly washed with distilled water and dissolved in a 9.3 M lithium bromide (LiBr) solution at 60 °C for one hour. The resulting silk solution underwent dialysis against distilled water at room temperature for 72 h to remove LiBr. The dialyzed silk solution was collected, centrifuged to eliminate any residual impurities, and stored in a refrigerator at 4 °C for later use.[2]

2.3 Preparation of TPU solution

15 g of TPU particles were dissolved in 100 ml of N, N-dimethylformamide (DMF) and stirred for 24 h to prepare a 15% (w/v%) TPU solution.

2.4 Construction of composite aerogel fibers

GO/SF@TPU aerogel fibers were prepared via coaxial wet-spinning. Graphene oxide (GO) suspension was incorporated into the pre-prepared silk fibroin protein (SF) solution and sonicated to ensure uniform dispersion, with a GO to SF ratio of 4:1. The mixed solution was stirred at room temperature for 48 h, with the concentration adjusted to 20 mg ml^{-1}. The GO/SF solution and the TPU solution were respectively loaded into separate syringes. Through a coaxial stainless-steel needle with an inner diameter of 1.05 mm (22G) and an outer diameter of 0.4 mm (17G), the mixture was extruded into deionized water via coaxial wet-spinning and then frozen at-23 °C for 5 hours, followed by a 12-hour freeze-drying treatment.

3 Preparation of RGO/SF@TPU-PEG PCFs

GO/SF@TPU-PEG PCFs were synthesized via vacuum-assisted infiltration. Firstly, 15 g of PEG was heated to 90 °C and dissolved in 15 ml of deionized water to achieve a 50 wt.%, followed by vigorous stirring for 2 h. The prepared fibers were then infiltrated with the PEG solution, subjected to vacuum for 1 h, the excess liquid was removed by absorption using filter paper. Finally, the samples were left to dry thoroughly.4 Characterization

Mechanical properties were tested on an electronic universal testing machine (UTM2102). Optical photographs of the samples were taken with a Canon camera (EOSM6m2). Surface temperatures were measured using a HIKMICRO pyrometric thermal imaging camera. Freeze-drying with Vacuum Freeze-Dryer (LC-12N-50A)，

The morphology and structure features were determined by scanning electron microscopy (SEM, TM4000),The chemical structure was characterized by X-ray diffractometer (XRD, Empyrean) and In-situ Fourier Transform Infrared Spectrometer (FTIR, Nicolet iS50).The phase change properties were investigated by differential scanning calorimeter (Discovery DSC, TA, America) under nitrogen atmosphere. The thermal conductivity measurements with an uncertainty of ± (2-5) % were performed on a thermal constants analyzer (Hot Disk) at room temperature. The thermal stability was determined using a thermogravimetric analyzer (TG, NETZSCH TG209) from room temperature to 800 °C with a heating rate of 10 °C min^{-1} under nitrogen

atmosphere. Mercury intrusion porosimetry (MIP) analysis uses a high-performance fully automatic mercury porosimeter (AutoPore 9620, USA).

Informed consent was obtained from all volunteers prior to conducting the thermal insulation experiments.

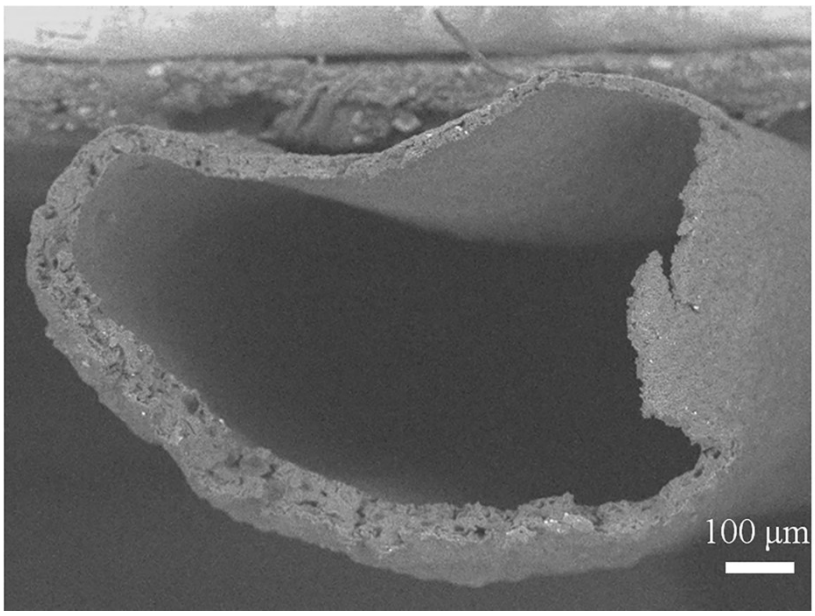

Figure S1. SEM image of cross section of Hollow TPU aerogel fibers.

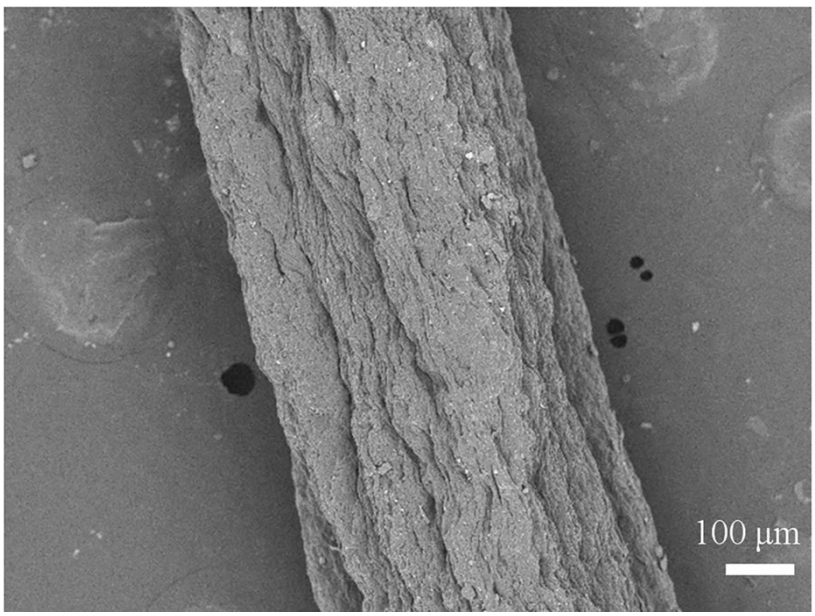

Figure S2. SEM image of surface of GO/SF@TPU aerogel fibers.

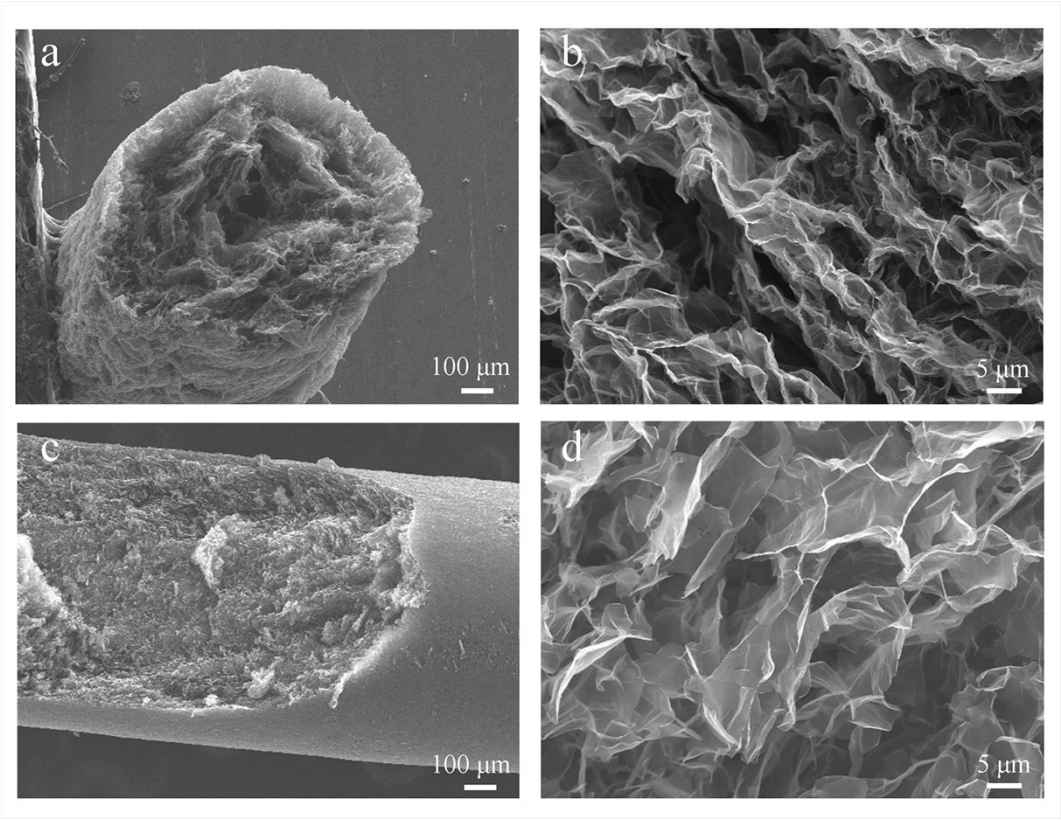

Figure S3. SEM image of surface of GO aerogel fibers. (a)-(b) Cross-sectional morphology and (c)-(d) longitudinal section morphology.

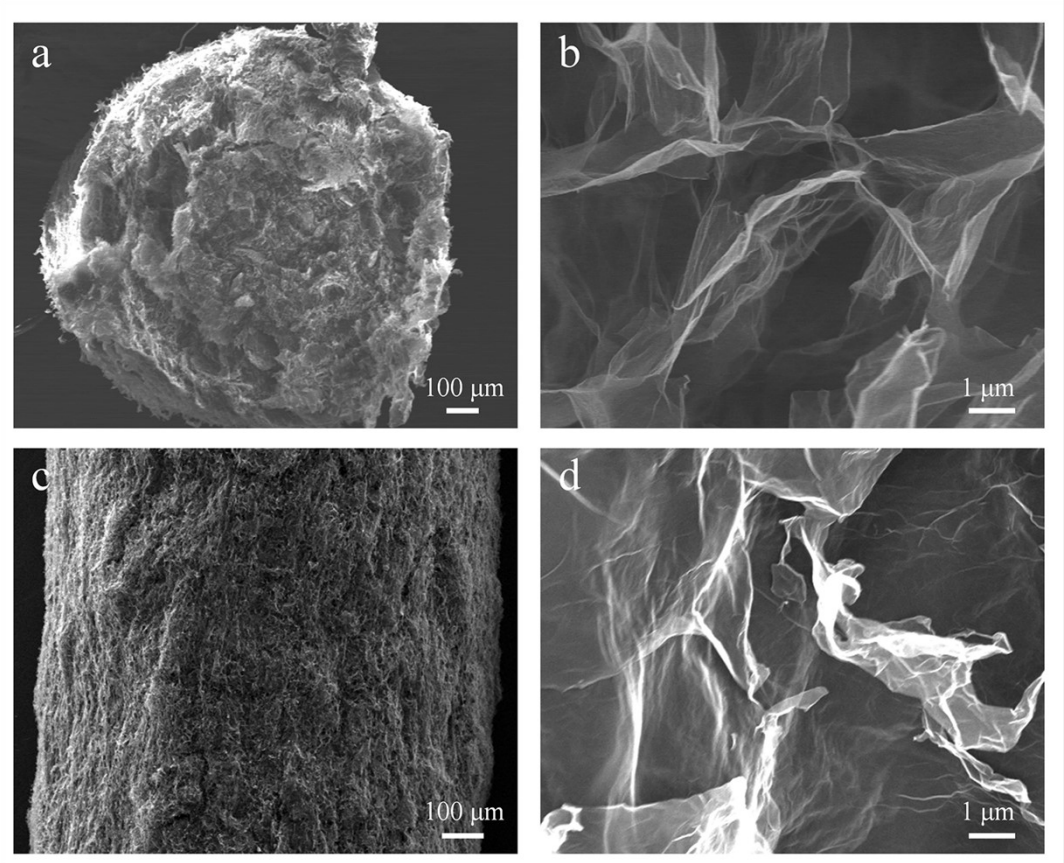

Figure S4. SEM image of surface of GO/SF aerogel fibers. (a)-(b) Cross-sectional morphology and (c)-(d) surface topography.

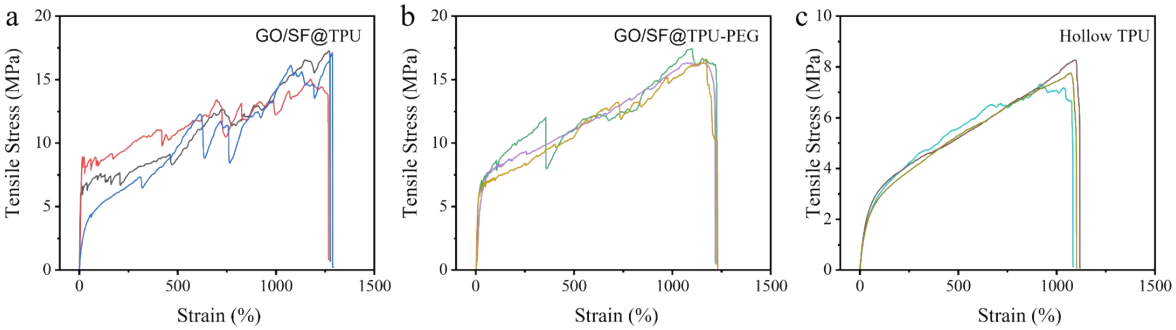

Figure S5. Stress-strain curves of GO/SF@TPU aerogel fibers (a), GO/SF@TPU-PEG aerogel fibers (b), and hollow TPU aerogel fibers (c).

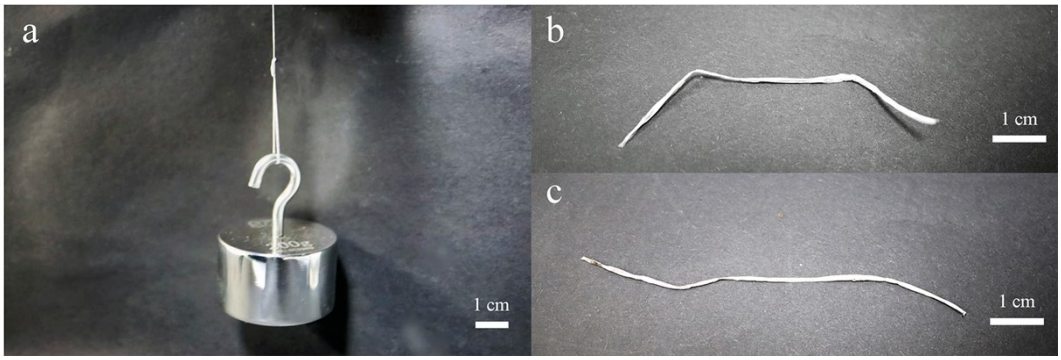

Figure S6. a. Diagram depicting a single GO/SF@TPU aerogel fiber lifting a 200 g weight. Before (b) and after (c) the fiber lifts the weight.

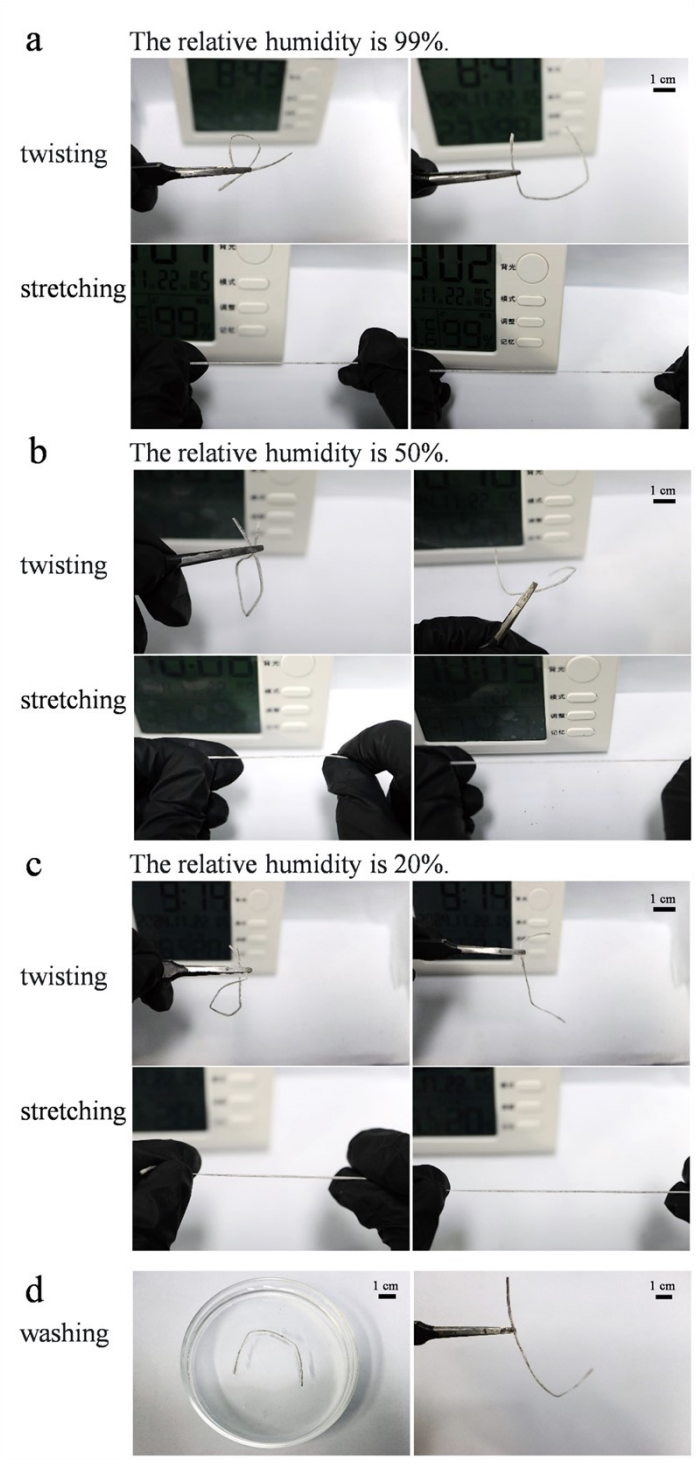

Figure S7. Optical images of the same GO/SF@TPU aerogel fibers twisting, stretching, and washing processes that demonstrate the shape stability of aerogel fibers. a. Twisting and stretching at 99% humidity. b. Twisting and stretching at 50% humidity. c. Twisting and stretching at 20% humidity. d. washing.

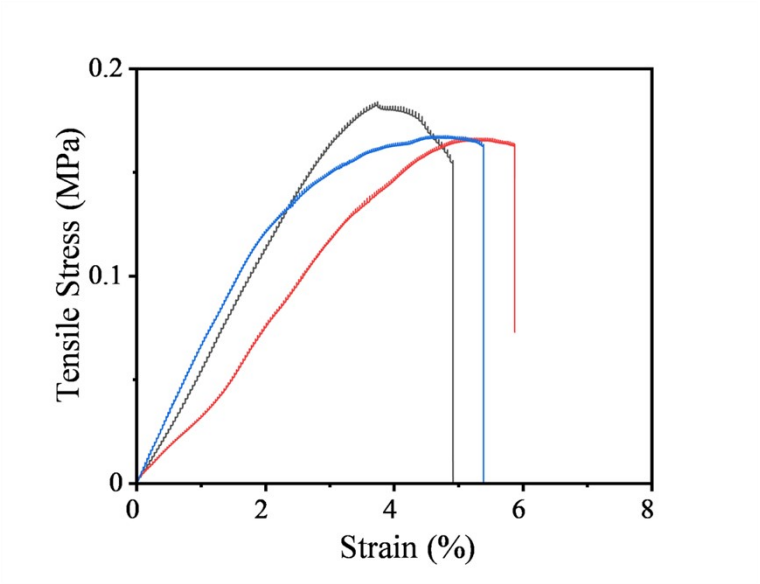

Figure S8. Stress-strain curves of GO/SF aerogel fibers.

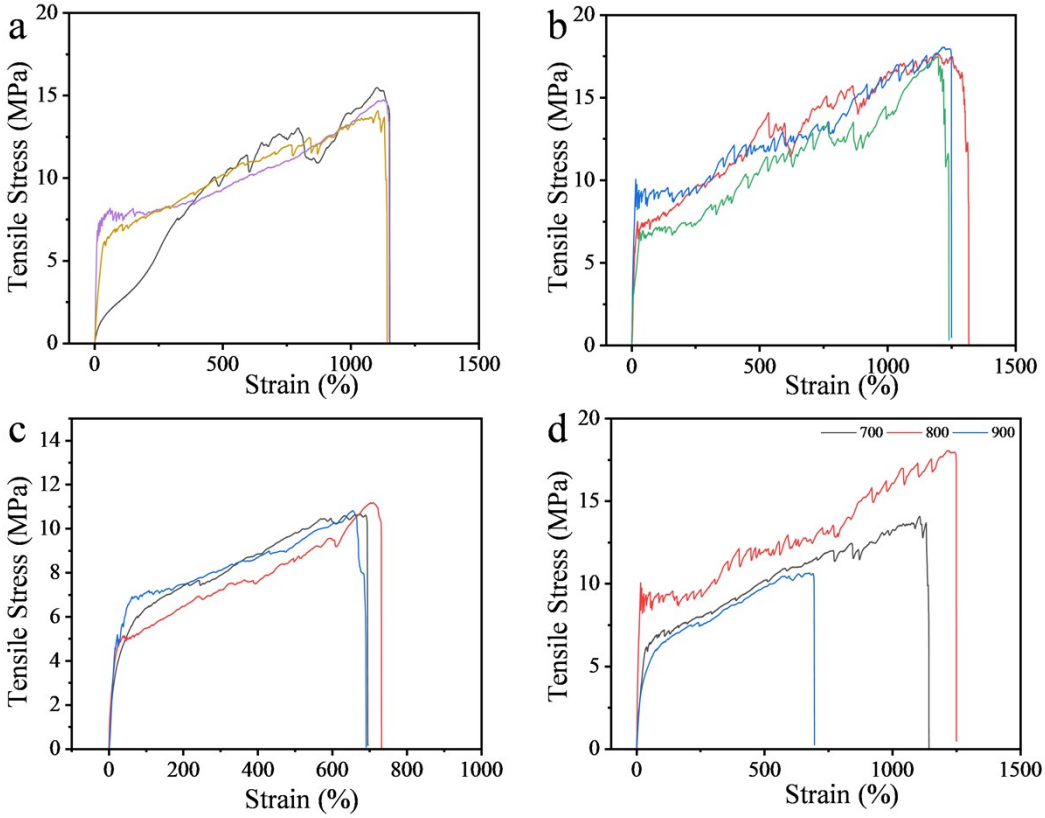

Figure S9. Stress-strain curves of aerogel fibers prepared with an outer flow rate of 300 ul min^{-1} and inner flow rates of 700 ul min^{-1} (a), 800 ul min^{-1} (b), and 900 ul min^{-1} (c), respectively, and contrast (d).

The colored lines in Figures S5, S8 and S9 are multiple fibers of the same sample.

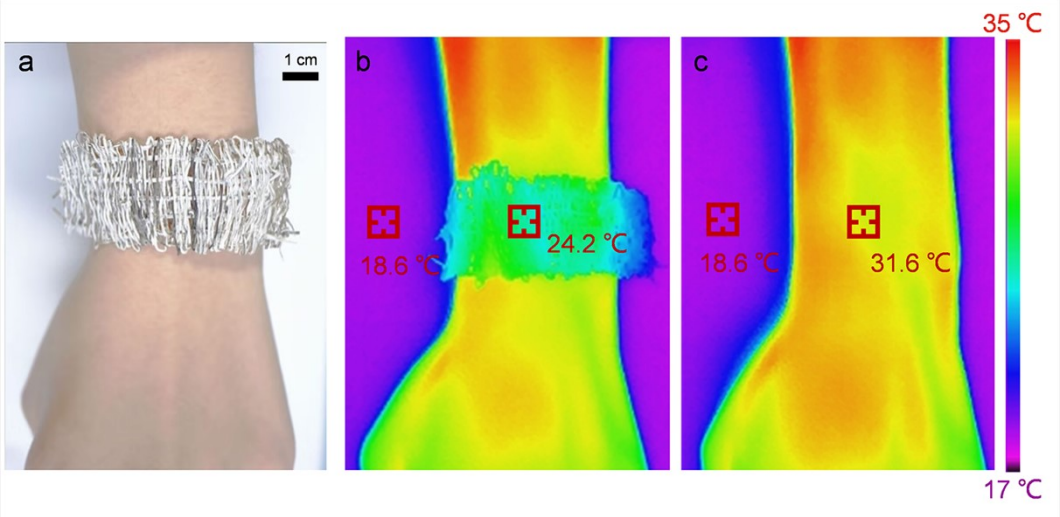

Figure S10. Thermal insulation tests of GO/SF@TPU fabric on human skin. (a) Optical images, (b) thermal images of the fabric surface, (c) thermal images of the skin surface.

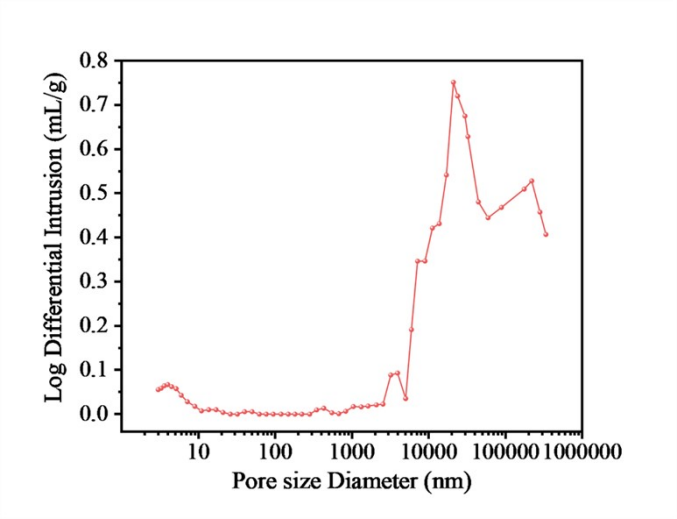

Figure S11. Pore size distribution of the GO/SF@TPU aerogel fibers from MIP analysis.

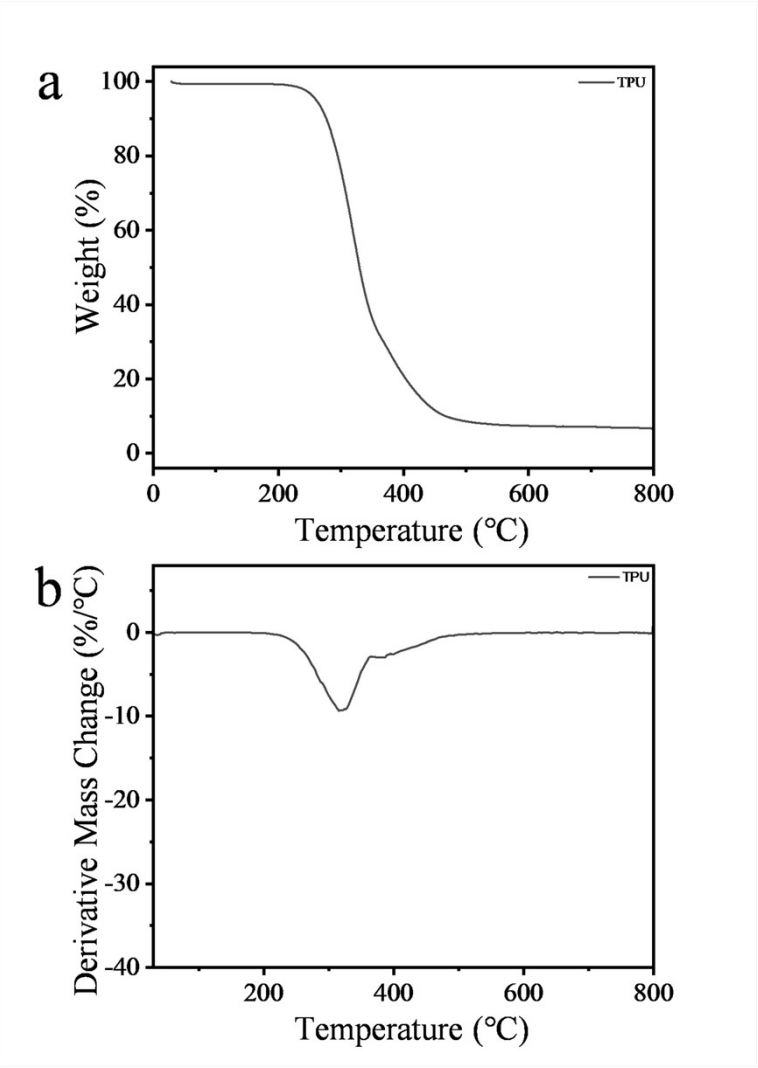

Figure S12. (a) TGA curves of Hollow TPU aerogel fibers. (b) DTG curves of Hollow TPU aerogel fibers.

Differential scanning calorimetry (DSC) analysis revealed a weight loss of 37.5% for TPU within the first stage (200-317°C), which may be attributed to the decomposition of lower molecular weight components, potentially encompassing both the soft segments and the thermally unstable parts of the hard segments. The second stage (317-362°C) exhibited a weight loss of 30.7%, suggesting the degradation of higher molecular weight fractions along with possible decomposition of cross-linked structures. In the third stage (362-490°C), the sample lost an additional 8.9% of its weight, with a decreased rate of loss, likely due to the residual char formation or the presence of other thermally stable inorganic fillers.

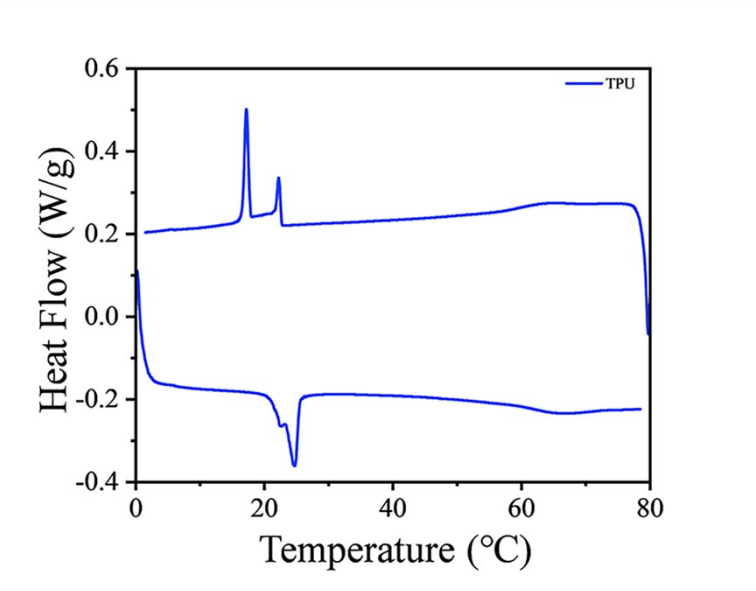

Figure S13. DSC curves of Hollow TPU aerogel fibers.

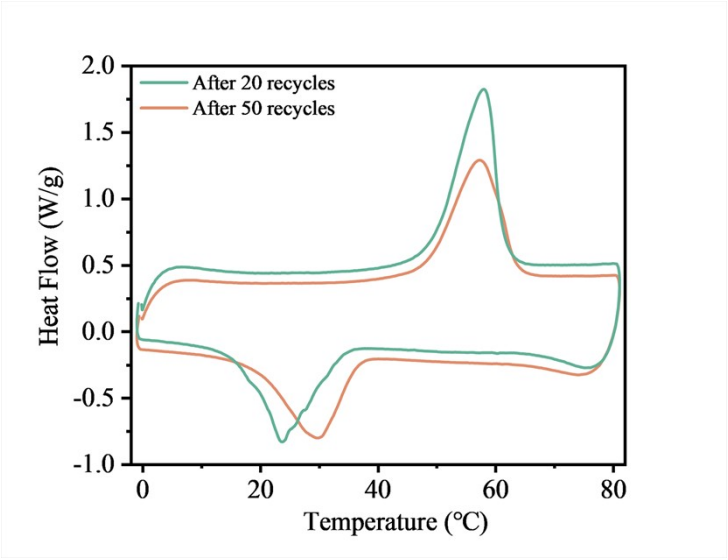

Figure S14. DSC curves of GO/SF@TPU-PEG PCFs after 20 times and 50 times thermal cycles.

$$\text{Toughness} = \int_0^{\epsilon_f} \sigma(\epsilon) d\epsilon \qquad \text{S(1)}$$

In the equation (S1), The lower limit of integration is 0, indicating the start of integration from zero strain.The upper limit of integration is ϵ f, indicating integration up to the strain at which the material fractures. $\sigma(\epsilon)$ is the stress as a function of strain.The geometric meaning of this integral is the area under the strain-stress curve, which represents the energy absorbed by the material before it fractures.

$$\alpha(\%) = \frac{m_{PCM}}{m_{total}} \times 100 \qquad \text{S(2)}$$

In the equation (S2), m_{PCM} refers to the mass of the phase change material (PCM), expressed in grams (g), while m_{total} represents the total mass of the composite material, also measured in grams (g).

$$R(\%) = \frac{\Delta H_{m,CPCM}}{\Delta H_{m,PCM}} \times 100 \qquad \text{S(3)}$$

In the equation (S3) $\Delta H_{m,CPCM}$ and $\Delta H_{m,PCM}$ are expressed as molten enthalpies of composite PCMs and PCM, respectively.

Table S1. The mechanical properties of the different fibers

Fiber Sample	Tensile strength (MPa)	Toughness (MJ m^{-3})
GO/SF	0.16±0.0049	0.0054±0.0016
700 ul min^{-1}	14.53±0.97	114.88±3.69
800 ul min^{-1}	17.58±0.27	154.61±17.12
900 ul min^{-1}	10.82±0.29	58.63±3.65
GO/SF@TPU	16.46±1.25	137.73±6.27
GO/SF@TPU-PEG	16.29±0.18	143.01±3.60
Hollow TPU	7.54±0.84	58.67±1.75

Table S2. TGA data of different materials.

Simple	T_0 (℃)	T_{max} (℃)	Residue (wt.%)
PEG	312	392	0.46
TPU	200	317	8.1
GO/SF@TPU-PEG	226	392	8.38

Table S3. Enthalpies of different simples.

Simple	Tm (°C)	ΔH m (J g^{-1})	Tc (°C)	ΔH c (J g^{-1})
PEG	57.33	198.47	41.38	176.04
GO/SF@TPU-PEG	51.57	86.66	33.82	69.84
GO/SF@TPU-PEG after 20 times cycles	49.1	66.07	35.5	44.62
GO/SF@TPU-PEG after 50 times cycles	48.4	53.05	38.2	40.35

Table S4. Comparison between the aerogel fibers in this work and other reported aerogel fibers.

Simple	Stress (MPa)	Toughness (MJ m^{-3})	Thermal Conductivity (W m^{-1} K^{-1})	Latent heat (J/g)	Density (g/cm^3)	Specific (J/g K)	Thermal diffusivity (mm^2/s)	Ref.
PI	11.00	1.890	0.0320	-	-	-	-	3
EAF	12.70	95.80	0.0260	-	-	-	-	4
Biomimetic Fiber	0.950	0.4200	0.0220	-	-	-	-	5
CA/PAA@CNF	5.830	0.6200	0.0540	-	-	-	-	6
PVA aerogel fibers	8.360	2.290	0.0260	-	-	-	-	7
Polyimide aerogel fibers	5.200	0.4900	0.0287	-	0.230	-	-	8
Kevlar aerogel fiber	3.300	0.6900	0.0370	-	-	-	-	9
HZAFs	8.600	0.001900	0.0360	-	0.120	-	-	10
Transparent silica aerogel fibers	0.300	0.1300	0.0230	-	0.160	-	-	11
NKLC aerogel fibers	41.00	5.340	0.0370	-	-	-	-	12
LPF-PAF	17.00	0.7900	0.0367	-	0.350	-	-	13
ANFs/mCNTs	4.400	5.9000	0.0600	-	0.00751			14
mTPU-SA	10.26	0.2100	0.0240	-	0.140	-	-	15
LCNF aerogel	0.960	0.0140	0.0530	-	-	-	-	16
BGC@C_{18}4 aerogel	0.065	0.001900	0.0440	195.0	-	-	-	17
MF-GO aerogel	0.140	0.0860	0.0270	-	-	-	-	18
SixPRA-y	1.140	0.0360	0.0330	-	0.0580	-	-	19
CTA	0.140	0.1100	0.0230	-	8.20	-	-	20
CoNA-05	0.051	1500	0.0442	-	0.0700	-	-	21
Cotton Fiber	525.0	0.7800	0.0730	-	1.50	-	-	22
Wool Fiber	195.0	7.480	0.0530	-	1.30	-	-	22
Silk Fiber	518.0	21.93	0.0520	-	1.40	-	-	22
Polyester fiber	630.0	18.99	0.0840	-	1.40	-	-	22
Nylon fiber	581.0	17.13	0.3370	-	1.10	-	-	22
PIA0	5.580	1.390	0.0047	-	-	-	-	23
PIA2	5.660	2.070	0.0031	-	-	-	-	23
MGF/GF/PDM	1.565	0.0791	1.080	-	-	-	-	24

S								
PMFs	28	-	-	91.00	-	-	-	[25]
paraffin/graphene	-	-	0.75	203.0	-	-	-	[26]
paraffin/MWCNTs composite PCMs	-	-	0.61	198.0	-	-	-	[26]
GO/SF@TPU	17.21	136.8	0.0826	-	0.597	0.377	0.368	This Work
GO/SF@TPU-PEG	16.07	142.3	0.0863	86.66	0.843	0.522	0.197	This Work

References

1. W. S. Hummers, Jr. and R. E. Offeman, *Journal of the American Chemical Society*, 1958, **80**, 1339-1339.
2. S.-D. Wang, Q. Ma, K. Wang and P.-B. Ma, *International Journal of Biological Macromolecules*, 2018, **111**, 237-246.
3. X. Li, G. Dong, Z. Liu and X. Zhang, *ACS Nano*, 2021, **15**, 4759-4768.
4. M. Wu, Z. Shao, N. Zhao, R. Zhang, G. Yuan, L. Tian, Z. Zhang, W. Gao and H. Bai, *Science*, 2023, **382**, 1379-1383.
5. Y. Cui, H. Gong, Y. Wang, D. Li and H. Bai, *Advanced Materials*, 2018, **30**, 1706807.
6. H. Sun, W. Mu, X. Cui, Z. Xu, T. Zhang and Y. Zhao, *ACS Applied Polymer Materials*, 2023, **5**, 552-559.
7. Y. Liu, Y. Zhang, X. Xiong, P. Ge, J. Wu, J. Sun, J. Wang, Q. Zhuo, C. Qin and L. Dai, *Macromolecular Materials and Engineering*, 2021, **306**, 2100399.
8. T. Xue, C. Zhu, X. Feng, Q. Wali, W. Fan and T. Liu, *Advanced Fiber Materials*, 2022, **4**, 1118-1128.
9. Z. Liu, J. Lyu, D. Fang and X. Zhang, *ACS Nano*, 2019, **13**, 5703-5711.
10. P. Hu, F. Wu, B. Ma, J. Luo, P. Zhang, Z. Tian, J. Wang and Z. Sun, *Advanced Materials*, 2024, **36**, 2310023.
11. Y. Du, X. Zhang, J. Wang, Z. Liu, K. Zhang, X. Ji, Y. You and X. Zhang, *ACS nano*, 2020, **14**, 11919-11928.
12. Z. Liu, J. Lyu, Y. Ding, Y. Bao, Z. Sheng, N. Shi and X. Zhang, *ACS Nano*, 2022, **16**, 15237-15248.
13. C. Zhu, T. Xue, Z. Ma, W. Fan and T. Liu, *ACS Applied Materials & Interfaces*, 2023, **15**, 12443-12452.
14. M. Li, X. Chen, X. Li, J. Dong, C. Teng, X. Zhao and Q. Zhang, *Composites Communications*, 2022, **35**, 101346.
15. H. Omranpour, S. Hassanifard, A. R. Monfared, B. O. Shahreza, A. Salehi, A. Jalali, M. Kheradmandkeymousi, S. S. Rahman, K. Behdinan and C. B. Park, *Advanced Composites and Hybrid Materials*, 2024, **7**, 105.
16. C. Liu, M.-C. Li, X. Liu, G. Zhou, C. Liu and C. Mei, *Additive Manufacturing*, 2023, **78**, 103841.
17. Y. Li, X. Zhao, Y. Tang, X. Zuo and H. Yang, *Advanced Functional Materials*, **n/a**, 2403059.
18. L. Wang, J. Wang, L. Wu and X. Wang, *Composites Part A: Applied Science and Manufacturing*, 2021, **140**, 106195.
19. H. Huang, Y. Lv, X. Jin, H. Wang, C. Wu, Y. Pan, X. Yan, C. Hong, W. Han and X. Zhang, *Chemical Engineering Journal*, 2023, **470**, 144413.
20. H.-J. Zhan, K.-J. Wu, Y.-L. Hu, J.-W. Liu, H. Li, X. Guo, J. Xu, Y. Yang, Z.-L. Yu, H.-L. Gao, X.-S. Luo, J.-F. Chen, Y. Ni and S.-H. Yu, *Chem*, 2019, **5**, 1871-1882.
21. J. Qi, Y. Xie, H. Liang, Y. Wang, T. Ge, Y. Song, M. Wang, Q. Li, H. Yu, Z. Fan, S. Liu, Q. Wang, Y. Liu, J. Li, P. Lu and W. Chen, *ACS Sustainable Chemistry & Engineering*, 2019, **7**, 9202-9210.
22. Y. Dongwei, *Textile Materials Science*, China Textile Publishing House, 2009.01.
23. Y. Liu, D. Wang and J. Li, *Frontiers in Materials*, 2023, **10**.
24. Y.-H. Zhao, Y.-F. Zhang and S.-L. Bai, *Composites Part A: Applied Science and*

Manufacturing, 2016, **85**, 148-155.

25. H. Liu, X. Zhang, S. Zhang, Y. Kou, H. Fu, F. Zhou, Z. S. Wu and Q. Shi, *Angewandte Chemie International Edition*, 2024, DOI: 10.1002/anie.202408857.
26. D. Zou, X. Ma, X. Liu, P. Zheng and Y. Hu, *International Journal of Heat and Mass Transfer*, 2018, **120**, 33-41.